Silk Fibroin and Functionalized Multiwall Carbon Nanotubes Hydrogels and Their Biomineralization Potential

CATALIN ZAHARIA, MIHAELA-RAMONA TUDORA, CELINA MARIA DAMIAN, EUGENIU VASILE, PAUL OCTAVIAN STANESCU*
[1]University Politehnica of Bucharest, Advanced Polymers Materials Group, 149 Calea Victoriei, 010072, Bucharest, Romania

The present work reports on the synthesis and biomineralization capacity of hydrogel networks composed of Bombyx mori silk fibroin, polyacrylamide and carboxylated multiwall carbon nanotubes soaked in simulated body fluid. Hydrogels were fabricated by the polymerization of acrylamide and N,N'-methylenebisacrylamide in silk fibroin solution containing carboxylated multiwall carbon nanotubes with potassium persulphate/ triethanol amine redox system as initiator. The incorporation of the fibroin and MWCNT-COOH within the polymer network was proved by FTIR spectroscopy. Swelling measurements in saline solution were performed to evaluate the behaviour of these hydrogels having various compositions. Biomineralization assays in simulated body fluid solution showed the presence of apatite-like crystals onto the surface of the materials. Beneficial effects upon biomeralization process of the carboxylated nanotubes were further discussed. Mechanical compressive tests revealed good strengths for the silk hydrogels depending on their composition. The results of this study lay down the fundament for the use of these silk fibroin biomaterials in bone tissue engineering applications.

Keywords: silk fibroin, carbon nanotubes, biomineralization, apatite, compressive strength

The development of biomaterials for tissue engineering has been focused on the design of protein-based scaffolds that can promote tissue regeneration. A synthetic polymer coated with bone-like apatite on its surface is likely to be useful as a scaffold for bone regeneration, since apatite is a major inorganic component of natural bone, and exhibits good biocompatibility and osteoconductivity [1]. Various methods were employed for coating the surface of the biomaterials with apatite [2-8]. Taguchi et al. proposed an alternate soaking process [7-8] in which a substrate is alternately soaked in calcium ion and phosphate ion solutions. The apatite formed by this process is quite different from bone apatite in its composition and structure. Apatite that is similar to bone apatite can be obtained if it is deposited from a simulated body fluid (SBF) [2-6] with ion concentrations approximately equal to those of human blood plasma.

Silk, popularly known in the textile industry for its luster and mechanical properties, is produced by cultured silkworms [9-10]. Silkworm silk from *Bombyx mori* is one of the most characterized silks and consists of heavy and light chains that form fibers with impressive mechanical strength [10-12]. Silks are high molecular weight block copolymers consisting of a heavy (~370 kDa) and a light (~26 kDa) chain with varying amphiphilicity linked by a single disulfide bond [6, 9-12]. These natural silkworm proteins have a highly repetitive amino acid sequence mainly composed of glycine (43%), alanine (31%), and serine (12%) residues [6, 9, 12-14]. The particular sequence of these amino acids with small side chains leads to the formation of hydrophobic domains, thus allowing the formation of thick packs of hydrogen bonded anti-parallel β-sheets [12-14]. Aqueous processing conditions, biocompatibility, good water vapour and oxygen permeability and biodegradability of silk fibroin, along with facile chemical modifications, are attractive features for its use as biomaterial [15].

Literature reviews related to silk reveal the long-standing use of this material as sutures [6, 12-15]. Silks can be processed into gels, films, fibers or sponges, all suitable for various biomedical applications [6, 15]. Therefore, silk fibroin is a suitable material for use in bone tissue engineering where mechanical strength and a slow degradation rate could be valuable attributes.

Silk hydrogels have been thoroughly studied for potential biotechnological and biomedical applications [6, 16-17]. To improve the properties of hydrogels, silk fibroin has been blended with various other polymers, which includes synthetic polymers such as polyvinyl alcohol as well as natural macromolecules like gelatin, collagen, elastin, etc [6, 16-19]. In a previous work [6] we have reported the synthesis and complex characterization of silk fibroin/ polyacrylamide hydrogels for tissue engineering applications. The present study focuses on the development of silk fibroin hydrogels and polyacrylamide reinforced with carboxylated multiwall carbon nanotubes. Mineralization behaviour of these biomaterials revealed the beneficial effect of carboxylated carbon nanotubes within the matrix. Compressive strengths were further improved as compared to previous results on silk fibroin/polyacryalmide hydrogels.

Experimental part

Materials and methods

The domesticated silkworm *(Bombyx mori* silk - *Lepidoptera: Bombycidae family)*, cocoons were kindly supplied by S.C. SERICAROM SA (Bucharest, Romania). Acrylamide (AAm) was purified by recrystallization from water and dried in air. N,N'-methylenebisacrylamide (MBA), potassium persulphate (KPS) and triethanol amine (TEA) were purchase from Sigma-Aldrich. Lithium bromide (LiBr), sodium bicarbonate and sodium dodecyl sulphate (SDS) were provided by Alfa Aesar GmbH&Co KG, Germany, while dialysis tubing cellulose membrane by Sigma-Aldrich. Multiwall Carbon Nanotubes (MWCNTs) were purchased from Sigma-Aldrich having more than 90 % carbon basis (trace metal basis) and O.D. x I.D. x L 10-15 nm x 2-6 nm x 0.1-10 μm, produced by Catalytic Chemical

* *email: paul_stanescu@yahoo.com; Tel.:0214022710*

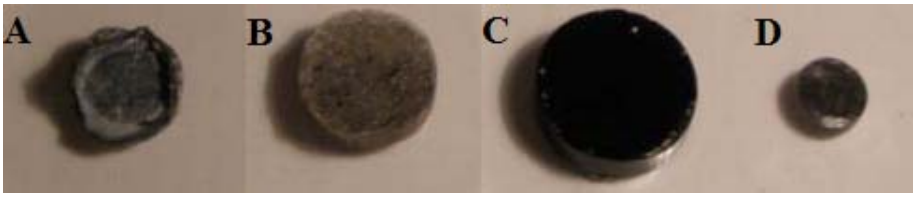

Fig. 1. SF/PAAm/MWCNT-COOH hydrogels: A) mineralized, B) lyophilized, C) swollen, D) dried

Vapour Deposition (CCVD), Arkema Inc. The oxidation process was made using a mixture of 98 % sulphuric acid (Merck) and 70 % nitric acid (Merck). The functionalization process of MWCNT was performed using a standard protocol [20].

Obtaining of silk fibroin solution

Bombyx mori silk cocoons were cut into pieces and then boiled for 30 min in 0.02 M Na_2CO_3 to separate the sericin proteins from the structural fibroin proteins. The fibroin extract was rinsed three times with bi-distilled water and dried for 24 h at 40 °C, followed by dissolving in 9.5 M LiBr solution at 65°C for 8 h. The solution was dialyzed against bi-distilled water using dialysis tubes (molecular weight cut-off, MWCO, 12.4 kDa) for 4 days. Prior to use the silk solution was filtered to remove any precipitate. The final concentration of aqueous silk solution was determined (via dehydration and weighing) to be 3.5 wt. %.

Obtaining of silk fibroin/polyacrylamide/carboxylated multiwall carbon nanotubes hydrogels

Hydrogels of silk fibroin (SF), polyacrylamide (PAAm) and carboxylated carbon nanotubes (MWCNT-COOH) were obtained by free radical polymerisation. Briefly, an aqueous solution of 15 wt. % AA having 1 wt. % N,N'-MBA was prepared and then mixed with SF solution in which there were dispersed the functionalized carbon nanotubes (MWCNT-COOH) in various ratios. The blended solutions were placed in glass vials together with the redox initiating system composed of KPS and TEA. The polymerisation reaction was performed under nitrogen atmosphere at 40°C for 4 days. The as prepared hydrogel matrices were purified by repeated extraction with bi-distilled water for 4 days to remove the unreacted residual acrylamide.

Characterisation techniques

The FT-IR spectra were taken on a Jasco 4200 spectrometer equipped with a Specac Golden Gate attenuated total reflectance (ATR) accessory, using a resolution of 4 cm^{-1} and an accumulation of 60 spectra, in the 4000 - 400 cm^{-1} wavenumber region.

Swelling behaviour of the hydrogels was tested in saline solution at 37 °C as a function of composition. The swelling degree of the hydrogels was determined using the conventional gravimetric method:

$$SD=((M_t - M_0)/M_0)\cdot 100 \quad (1)$$

where M_t and M_0 denote the weight of the wet hydrogel at a predetermined time and the weight of the dry sample, respectively. At least three swelling measurements were performed for each hydrogel sample and average values were reported.

Morphological information including internal structure was obtained through the scanning electron microscopy (SEM) analysis of the gold-coated hydrogels. Hydrogel samples were frozen at - 50 °C followed by lyophilization. The analysis has been performed using a QUANTA INSPECT F SEM device equipped with a field emission gun (FEG) with a resolution of 1.2 nm and with an X-ray energy dispersive spectrometer (EDS)

Biomineralization behaviour of SF/PAAm/MWCNT-COOH hydrogels

The main requirement for an artificial material to bond the living bone tissue represents the formation of hydroxyapatite on its surface when implanted in the living bone. To test the ability to induce the formation of hydroxyapatite, one may resort to the use of a solution (SBF, simulated body fluid) that mimics only the inorganic composition of human body fluids [2-5]. Three samples of each hydrogel composition were incubated in synthetic body fluid (SBF1x) at *p*H=7.49, adjusted with tris(hydroxymethyl) aminomethane (Tris) and hydrochloric acid (HCl), for 14 days, in containers with 45 mL of the incubation medium at 37 °C. After incubation, the hydrogels were rinsed with bi-distilled water to remove any traces of salts from the surface and dried at 40 °C for 24 h. The composition of SBF1x is: Na^+: 142.19 mM, Ca^{2+}: 2.49 mM, Mg^{2+}: 1.5 mM, HCO_3^-: 4.2 mM, Cl^-: 141.54 mM, HPO_4^{2-}, 0.9 mM, SO_4^{2-}: 0.5 mM, K^+: 4.85 mM [2-6].

The presence of mineral deposits onto the surface of the hydrogels was evaluated by SEM analysis. The Ca/P molar ratio was investigated by EDS spectroscopy.

Mechanical analysis

Mechanical properties of SF/PAAm/MWCNT-COOH hydrogels were evaluated by unixial compression on an Universal Testing Machine equipped with Instron 3382 2kN cell force. The test speed of the crosshead was set at 1 mm/min. Data were collected for three specimens for each hydrogel composition with 0.5% accuracy of force measurement and position accuracy of 0.001 mm. Hydrogel disks (15±0.5 mm diameter and 4±0.2 mm height) with flat and parallel surfaces were prepared and were allowed to swell in saline water solution at 37 °C for 30 h before the test. Compressive strength and strain were determined for fully swollen hydrogel samples.

Results and discussions

Obtaining of SF/PAAm/MWCNT-COOH

Silk fibroin/polyacrylamide/MWCNT-COOH hydrogels were obtained by the polymerization reaction of acrylamide and N,N'-methylenebisacrylamide with redox initiator in silk fibroin solution containing dispersed functionalized carbon nanotubes (1 wt. % MWCNT-COOH).

The compositions of the hydrogel networks were as follows: 0/100, 10/90, 20/80, 30/70, 40/60, 50/50, 70/30 in volumetric ratios (SF/PAAm). The polymerisation and cross-linking reactions were almost complete after 4 days leading to three-dimensional polymeric networks where silk fibroin was physically entrapped (fig. 1). 70/30 composition was not furthermore studied due to low physical integrity.

FTIR-ATR characterisation of SF/PAAm/MWCNT-COOH hydrogels

The results of the FTIR-ATR spectra gave us the specific absorbance wavelengths of the specific bonds which appeared in the silk fibroin/polyacrylamide/MWCNT-COOH

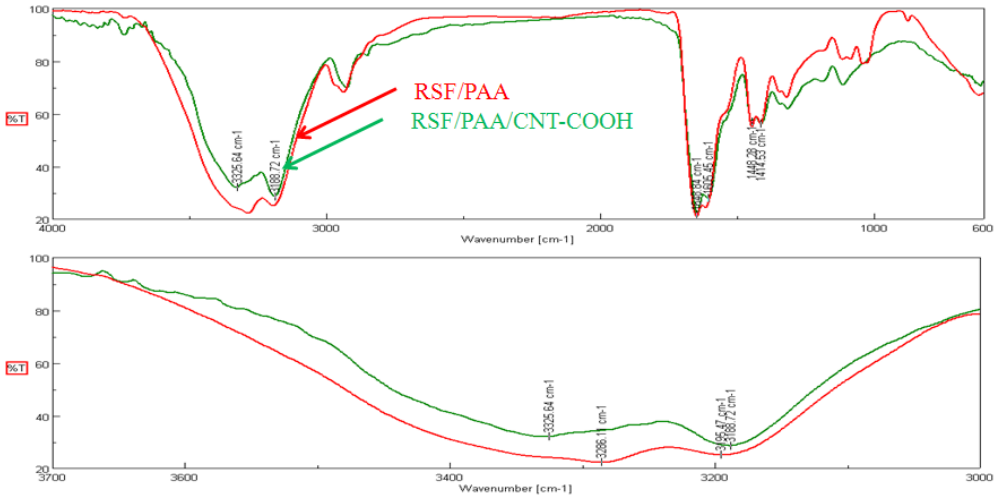

Fig. 2. FTIR-ATR spectra for SF/PAAm (10/90 v/v), and SF/PAAm/MWCNT-COOH (10/90 v/v)

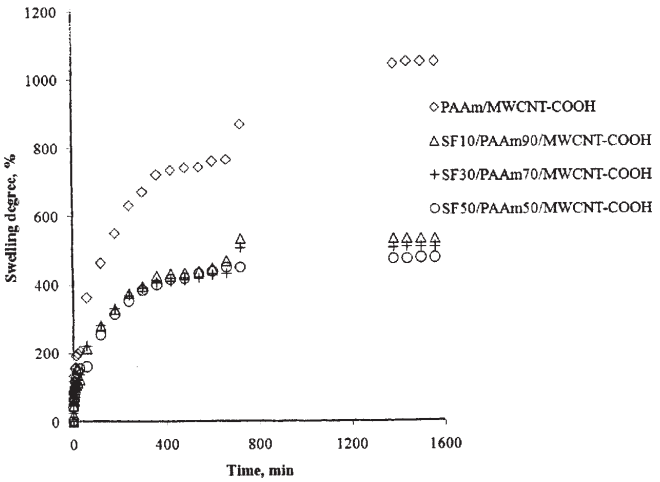

Fig. 3. Swelling degrees in saline solution at 37°C for SF / PAAm / MWCNT-COOH hydrogels

hydrogels, confirming the structure of the new materials (fig. 2). Typical peaks of silk fibroin are 1621, 1515 and 1231 cm^{-1}, characteristic for amide I (C=O stretching), amide II (NH deformation and C–N stretching) and amide III (C–N stretching and N–H deformation) [6]. In the case of polyacrylamide, there is a peak with two spikes assigned to N-H stretch and a strong C=O stretch having also two spikes (1648 and 1605 cm^{-1}). The FTIR analysis of the hydrogels confirmed the spectral modification as a function of composition. The presence of carbon nanotubes is hardly revealed by FTIR analysis, even those functionalized with COOH groups (due to overlapping with the silk fibroin band). However we can see a slight peak shifting toward left of the signal from 3286 cm^{-1} in the hydrogel without nanotubes (silk fibroin-polyacrylamide 10/90, v/v) to 3385 cm^{-1} (SF/PAAm/MWCNT-COOH, 10/90 v/v).

Swelling behaviour of SF/PAAm/MWCNT-COOH hydrogels

Hydrogel properties depend strongly on the degree of cross-linking, the chemical composition of the polymer chains, and the interactions of the network and surrounding liquid. Figure 3 shows the water swelling behaviour of the SF/PAAm/MWCNT-COOH hydrogels. The water swelling occurred rapidly, reaching equilibrium of water uptake in about 24 h. The swelling degree increases with the decrease of the silk fibroin content within the hydrogel: SF/PAAm 0/100 composition showed a maximum swelling degree of 1050 %, SF/PAAm 10/90 - 540 %, SF/PAAm 30/70 - 510 % whereas the value of the swelling degree for SF/PAAm 50/50 was 477 %. This behaviour could be explained by the presence of the carbon nanotubes which acts as free-radical scavenger; however the presence of silk fibroin reduces the carbon nanotubes radical scavenger effect allowing the polymerization reaction to proceed under normal conditions.

Morphology of SF/PAAm/MWCNT-COOH hydrogels

SEM analysis showed the porous SF/PAAm/MWCNT-COOH hydrogels for various compositions with close and open-ended pores (fig. 4) and the nice carbon nanotubes dispersed in the hydrogel matrix.

Biomineralization behaviour of SF/PAAm/MWCNT-COOH hydrogels

The biomineralization capacity of SF/PAAm/MWCNT-COOH hydrogels was assessed through SEM analysis. All the hydrogels were uniformly covered with a mineral layer whose morphology does not depended on hydrogels composition (needle-like morphology for apatite crystals, fig. 5-7). Besides the effect of silk fibroin, the COOH groups of functionalized carbon nanotubes potentiate the effect of mineralization. Due to the use of constant concentrations of carbon nanotubes, the mineralization process is similar; the mineral deposition is uniform, with minor differences.

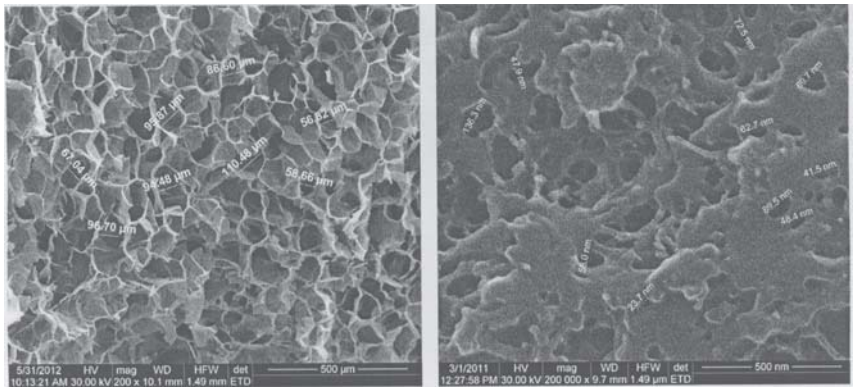

Fig. 4. SEM microphotographs for samples cross-section morphology revealing pores and carboxylated carbon nanotubes for SF/PAAm/MWCNT-COOH network (20/80, v/v)

Fig. 5. SEM microphotograph showing the apatite deposits onto the surface of SF/PAAm/MWCNT-COOH hydrogels (SF/PAAm 10/90, v/v), incubated in SBF 1x

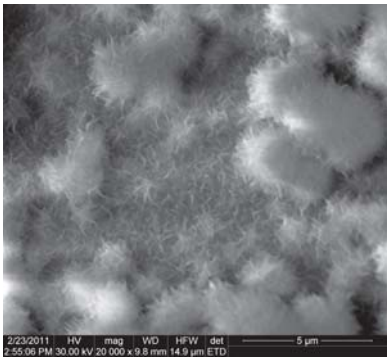

Fig. 6. SEM microphotograph showing the apatite deposits onto the surface of SF/PAAm/MWCNT-COOH hydrogels (SF/PAAm 30/70, v/v), incubated in SBF 1x

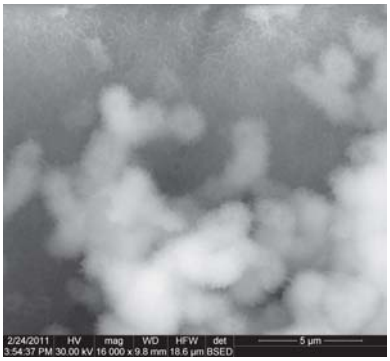

Fig. 7. SEM microphotograph showing the apatite deposits onto the surface of SF/PAAm/MWCNT-COOH hydrogels (SF/PAAm 50/50, v/v), incubated in SBF 1x

EDS analysis clearly identified Ca and P onto the surfaces of RSF/PAAm/MWCNT-COOH hydrogels (nanostructured HA crystals). The Ca/P molar ratios ranged between 1.5-1.7 for all the hydrogels.

Mechanical analysis

Compressive tests were performed on fully hydrated hydrogels specimens. Results of compressive strength for silk fibroin/polyacrylamide/MWCNT-COOH hydrogels with various compositions are shown in figure 8. Compressive strength of hydrogels shows a decreasing behaviour with the increase in fibroin content (fig. 8), but also the presence of the well dispersed carbon nanotubes resulted in a marked improvement of mechanical properties as compared to previously reported results [6].

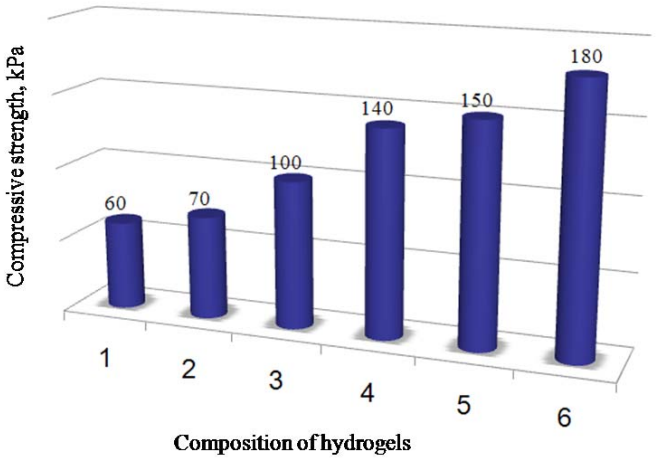

Fig. 8. Compressive strength diagram for full swollen SF/PAAm/MWCNT-COOH hydrogels with various compositions: SF/PAAm 1) 50/50, 2) 40/60, 3) 30/70, 4) 20/80, 5) 10/90, and 6) 0/100 v/v

Conclusions

Hydrogel networks of SF/PAAm/MWCNT-COOH with various compositions were obtained and characterized by physico-chemical and mechanical means. Apatite-like crystals were found onto the surfaces of silk fibroin/polyacrylamide/MWCNT-COOH hydrogels incubated in SBF1x. The presence of functionalized carbon nanotubes significantly improved the biomineralization behaviour of hydrogels in SBF1x, which no longer depends on the hydrogels composition, and also the presence of functionalized carbon nanotubes significantly improved the mechanical properties.

Next step should be the testing of the cytotoxicity of the materials on cell lines and *in vivo* tests that will clearly elucidate the capacity of the materials to initiate the formation of apatite crystals and to favour the osteo-conduction/osteoinduction phenomenon. The results of this study lay down the fundament for the use of these silk fibroin biomaterials in bone tissue engineering applications.

Acknowledgements: Authors recognise financial support from the European Social Fund through POSDRU/89/1.5/S/54785 project: "Postdoctoral Program for Advanced Research in the field of nanomaterials".

References

1.OYANE, A., UCHIDA, M., CHOONG, C., TRIFFITT, J., JONES, J., ITO, A., Biomaterials, **26**, 2005, p. 2407
2.KOKUBO T., ITO S., HUANG Z.T., HAYASHI T., SAKKA S., KITSUGI T., YAMAMURO T., J Biomed. Mater. Res., **24**, no. 3, 1990, p. 331
3.KOKUBO, T., KUSHITANI, H., SAKKA, S., KITSUGI, T., YAMAMURO, T., J. Biomed. Mater. Res., **24**, 1990, p. 721
4.KOKUBO T., TAKADAMA H., Biomaterials, **27**, no. 15, 2006, p. 2907
5. KOKUBO T., KIM H.M., KAWASHITA M., Biomaterials, **24**, no. 13, 2003, p. 2161
6.ZAHARIA, C., TUDORA, M.R., STANCU, I.C., GALATEANU, A., LUNGU, A., CINCU, C., Materials Science and Engineering C, **32**, 2012, pp. 945
7. TAGUCHI, T., KISHIDA, A., AKASHI, M., Chem Lett, **8**, 1998, p. 711
8.TAGUCHI T., MURAOKA Y., MATSUYAMA H., KISHIDA A., AKASHI M., Biomaterials, **22**, no. 1, 2001, p. 53
9.ALTMAN, G.H., DIAZ, F., JAKUBA, C., CALABRO, T., HORAN, R.L., CHEN, J., LU, H., RICHMOND, J., KAPLAN, D.L.,Biomaterials, **24**, 2003, p. 401
10.VEPARI, C., KAPLAN, D.L., Prog. Polymer Science, **32**, 2007, p. 991
11.HARDY, J.G., RÖMER, L.M., SCHEIBEL, T.R., Polymer, **49**, 2008, p. 4309
12.MONTI P., FREDDI G., BERTOLUZZA A., KASAI N., TSUKADA M., Journal of Raman Spectroscopy, **29**, no. 4, 1998, p. 297
13.MONTI P., TADDEI P., FREDDI G., ASAKURA T., TSUKADA M., Journal of Raman Spectroscopy, **32**, 2001, p. 103
14.LI, M., OGISO, M., MINOURA, N., Biomaterials, **24**, no. 2, 2003, p. 363
15.MIESZAWSKA, A.J., LLAMAS, J.G., VAIANA, C.A., KADAKIA, M.P.,. NAIK, RAJESH R., KAPLAN D.L., Acta Biomaterialia, **7**, 2011, p. 3036
16.MANDAL, B.B., KUNDU, C.S., Biomaterials, **30**, 2009, p. 2956
17.MANDAL, B.B., KAPOOR, S., KUNDU, S.C., Biomaterials, **30**, 2009, p. 2826
18.BALAKRISHNAN. B., AND BANERJEE, R., Chem Rev., **111**, no. 8, 2011, p. 4453
19.KUNDU, J., POOLE-WARREN, L.A., MARTENS, P., KUNDU, S.C., Acta Biomaterialia, **8**, 2012, p. 1720
20.DAMIAN, C.M., PANDELE, A.M., IOVU, H., U.P.B. Sci. Bull., Series B, **72**, no. 3, 2010, p. 164

Manuscript received: 25.03.2013